Electronic Supplementary Material (ESI) for Journal of Materials Chemistry B.
This journal is © The Royal Society of Chemistry 2020

Supplementary Information

A General Strategy of Designing NIR-II Emissive Silk for *In Vivo* Monitoring of Implanted Stent Model Beyond 1500 nm

Zhiming Deng[a,b], Junqing Huang[a,b], Zhenluan Xue[a], Mingyang Jiang[a], Youbin Li[a], Songjun Zeng*[a]

[a] School of Physics and Electronics, Key Laboratory of Low-dimensional Quantum Structures and Quantum Control of Ministry of Education, and Key Laboratory for Matter Microstructure and Function of Hunan Province, Hunan Normal University, Changsha, Hunan 410081, China.

[b] These authors contributed equally to this paper.

*Email: songjunz@hunnu.edu.cn.

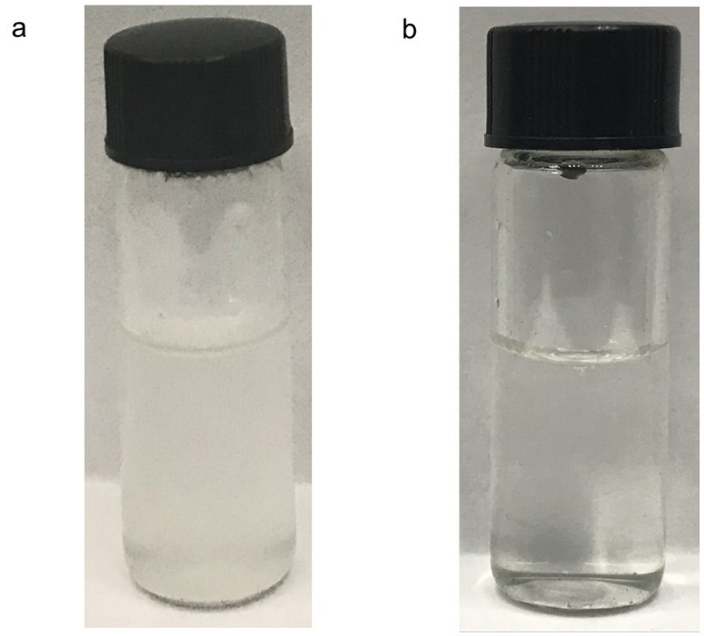

Figure S1. (a) Digital photo of $NaYF_4$ dispersed in cyclohexane and (b) $NaYF_4@SiO_2$ dispersed in water.

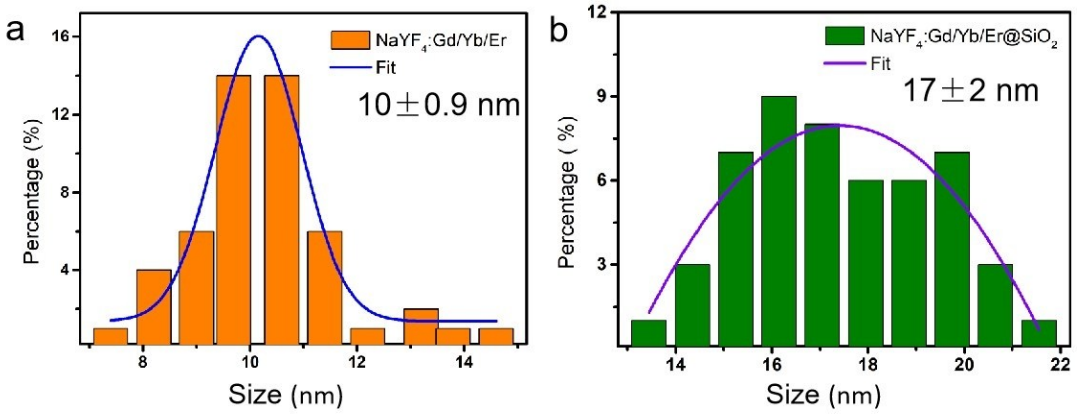

Figure S2. The size distribution histograms: (a) $NaYF_4$ and (b) $NaYF_4@SiO_2$ nanocrystals.

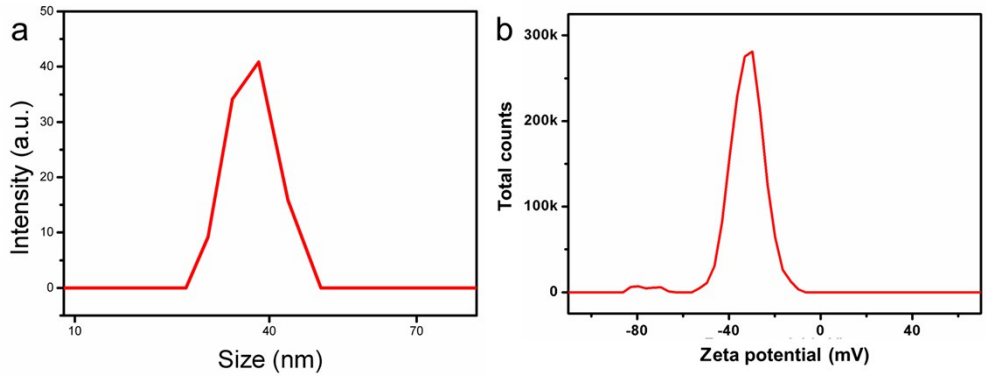

Figure S3. (a) Dynamic light scattering (DLS) measurement of the $NaYF_4$@SiO_2 nanocrystals. (b)The zeta potential distribution of the $NaYF_4$@SiO_2 nanocrystals.

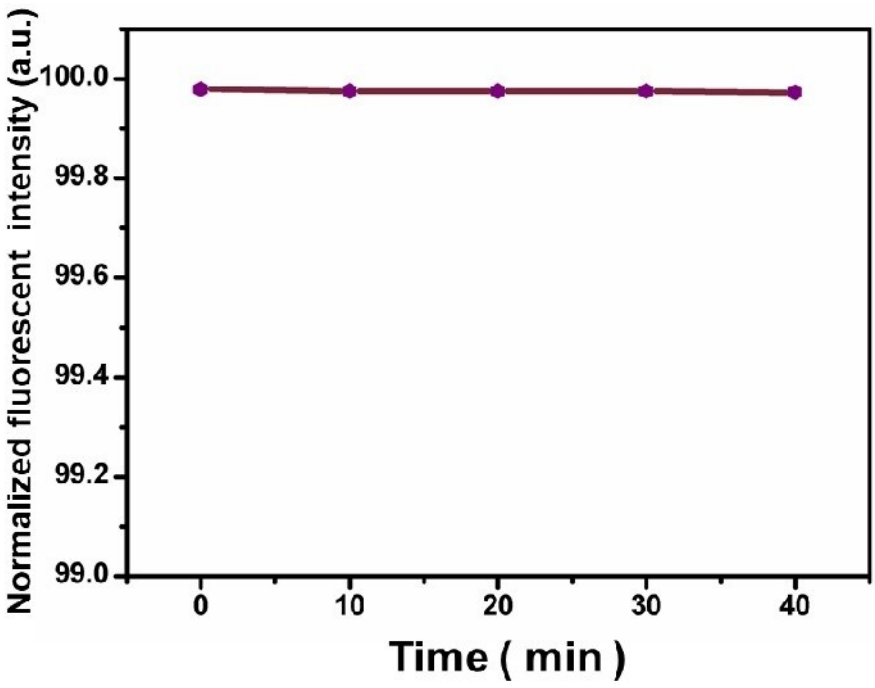

Figure S4. The photo-stability curve of the $NaYF_4$@SiO_2 in water under continuous 980 nm laser irradiation.

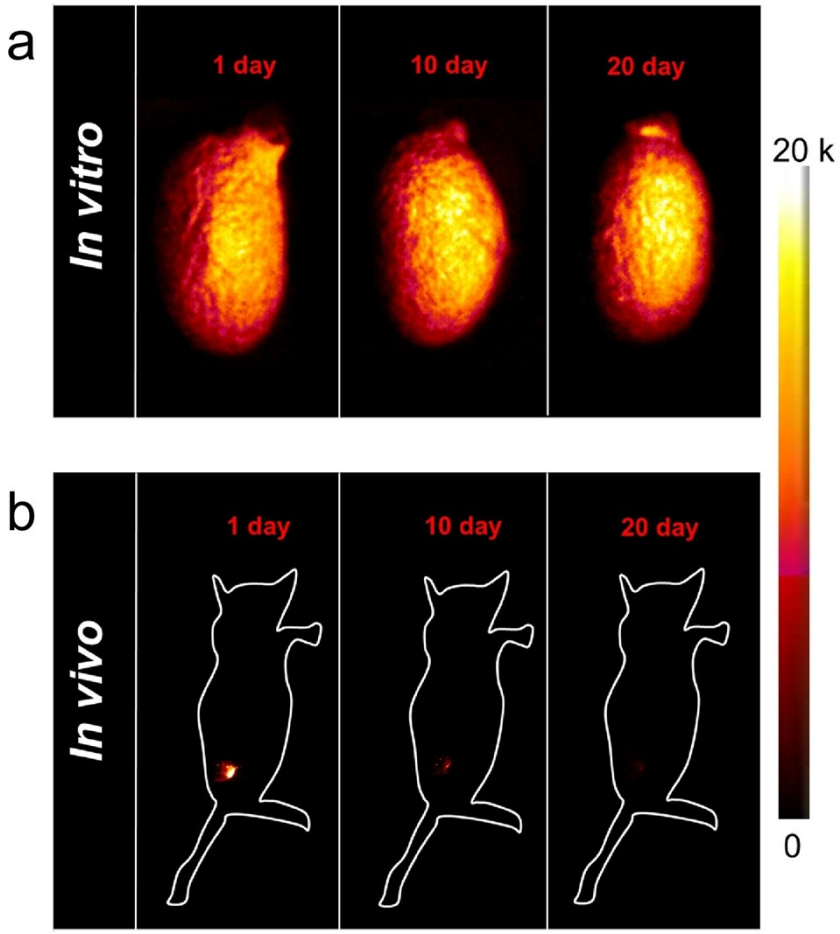

Figure S5. (a) *In vitro* and (b) *in vivo* optical stability of the $NaYF_4$-silk hybrid.

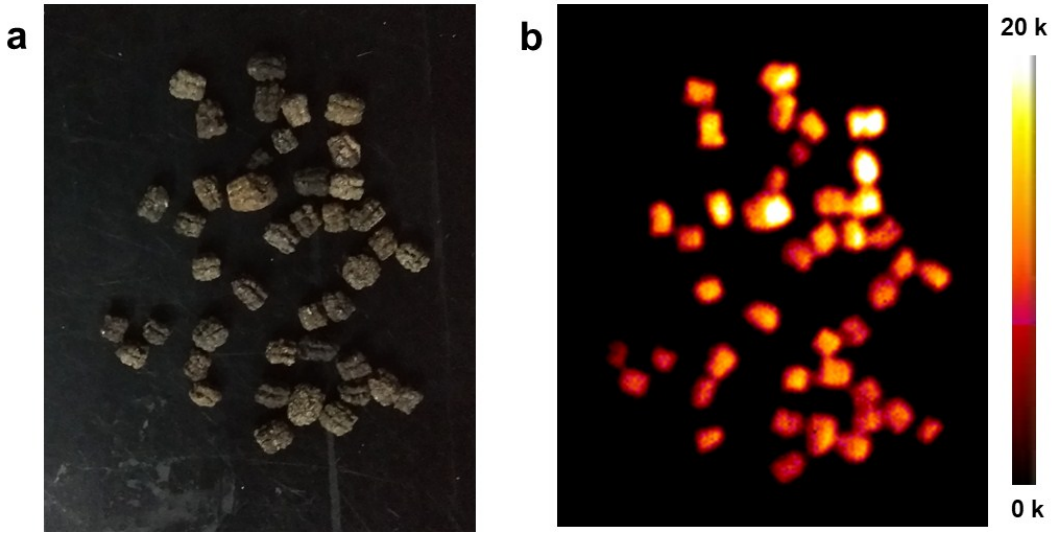

Figure S6. (a) Digital photograph and (b) the corresponding *in vitro* phantom imaging of the feces collected after feeding with $NaYF_4$@SiO_2.

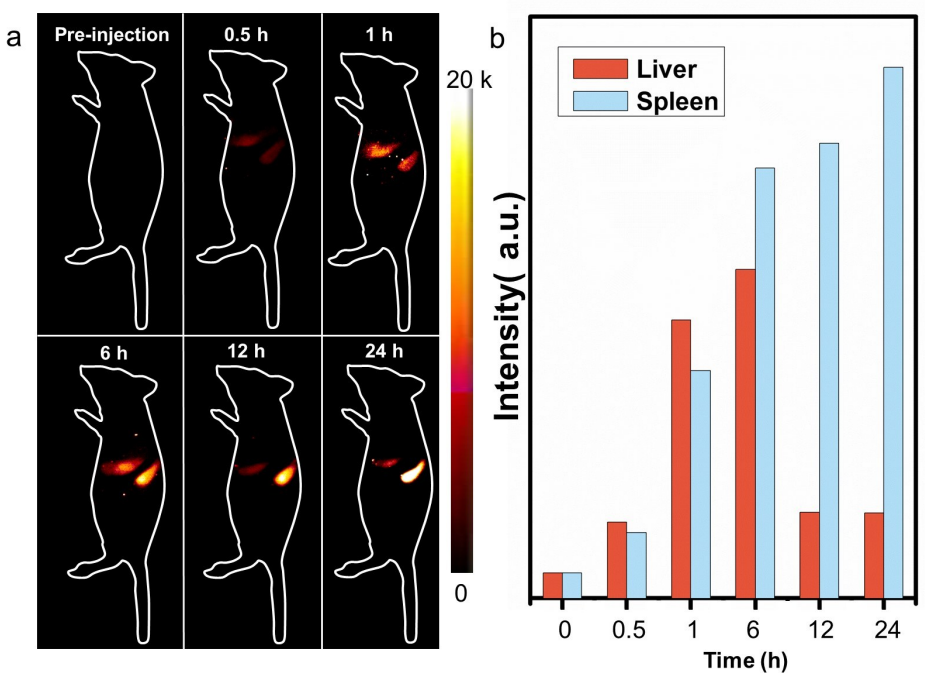

Figure S7. (a) *In vivo* NIR-II imaging and real-time tracking of mice after intravenous injection of $NaYF_4$@SiO_2 at different time intervals under 980 nm laser excitation. (b) The time-dependent NIR-II signal intensity change in the liver and spleen.

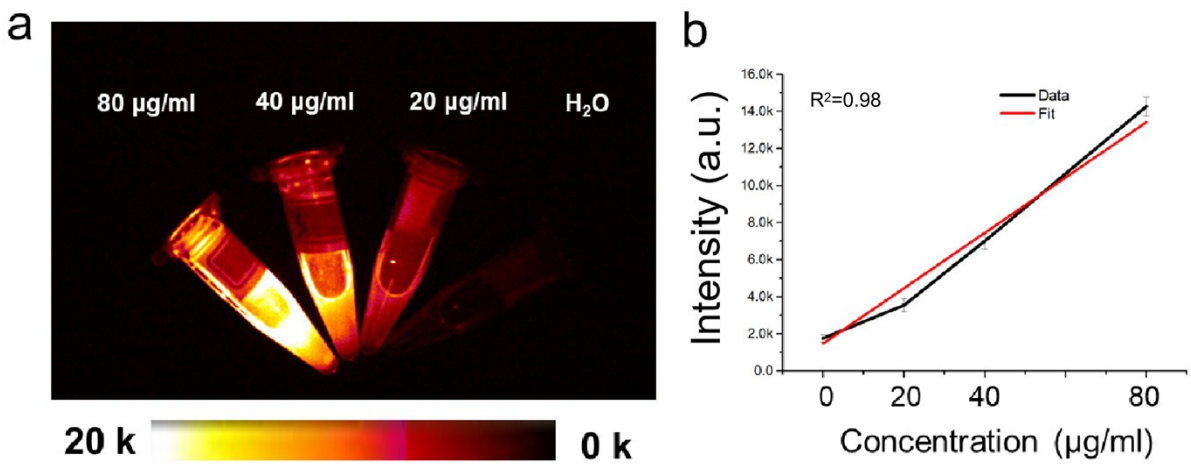

Figure S8. (a) The concentration-dependent NIR-II imaging of $NaYF_4$ nanoparticles. (b) The corresponding linearly fitting curve.

Table S1. ICP-MS (mg/kg) analysis of the $NaYF_4$-silk

Y	0.51	Au	<0.5	Co	<0.5	Li	<0.5	Pd	<0.5
Gd	0.85	B	<0.5	Cu	<0.5	Mg	416	S	1173
Yb	6.90	Ba	<0.5	Fe	<0.5	Mn	<0.5	Sb	<0.5
Er	1.01	Be	<0.5	Ga	<0.5	Mo	<0.5	Ti	<0.5
Si	21.8	Bi	<0.5	Ge	<0.5	Na	<0.5	V	<0.5
Ag	<0.5	Ca	2617	Hf	<0.5	Ni	<0.5	W	<0.5
Al	<0.5	Cr	<0.5	Hg	<0.5	P	<0.5	Zn	9.19
As	<0.5	Cd	<0.5	K	3059	Pb	<0.5	Zr	<0.5

Table S2. ICP-MS (mg/kg) analysis of the pure silk.

Y	<0.5	Au	<0.5	Co	<0.5	Li	<0.5	Pd	<0.5
Gd	<0.5	B	<0.5	Cu	<0.5	Mg	175	S	1402
Yb	<0.5	Ba	<0.5	Fe	<0.5	Mn	<0.5	Sb	<0.5
Er	<0.5	Be	<0.5	Ga	<0.5	Mo	<0.5	Ti	<0.5
Si	<0.5	Bi	<0.5	Ge	<0.5	Na	<0.5	V	<0.5
Ag	<0.5	Ca	2501	Hf	<0.5	Ni	<0.5	W	<0.5
Al	<0.5	Cr	<0.5	Hg	<0.5	P	<0.5	Zn	9.19
As	<0.5	Cd	<0.5	K	1636	Pb	<0.5	Zr	<0.5

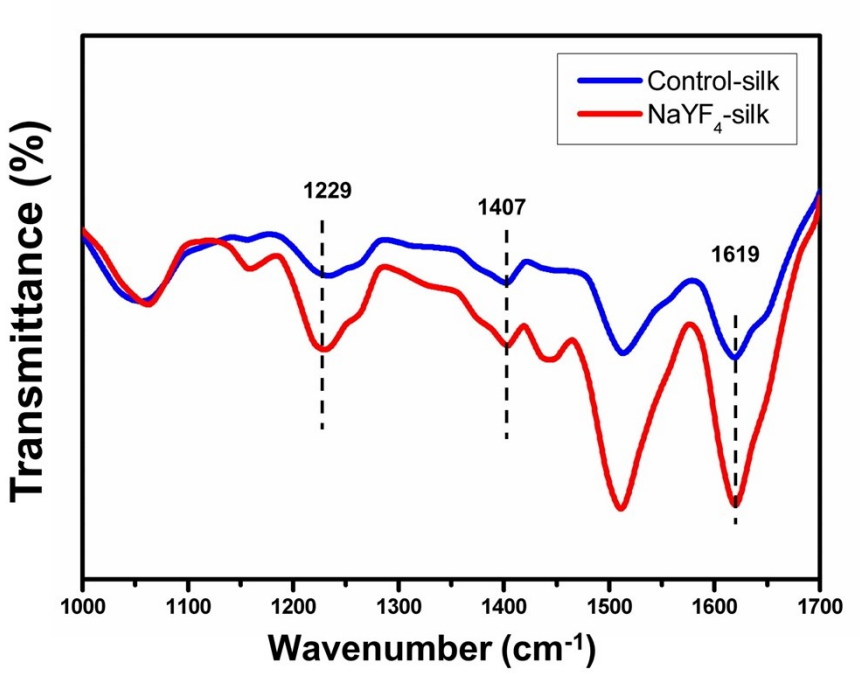

Figure S9. FTIR spectra of pure silk and $NaYF_4$-silk hybrids.

Table S3. Mechanical properties of silk fibers.

Sample	Pure Silk	$NaYF_4$-Silk
Tensile strength (MPa)	248.94	253.73

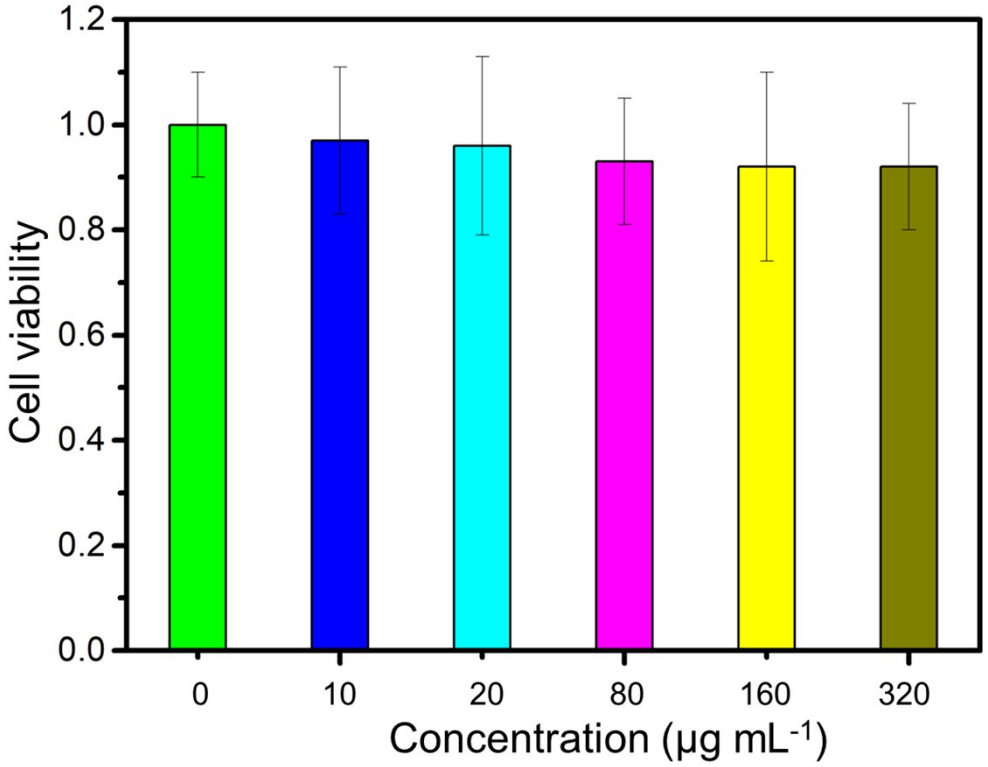

Figure S10. Viability of 4T1 tumor cells after treating with PBS solution of $NaYF_4@SiO_2$ at various concentrations.

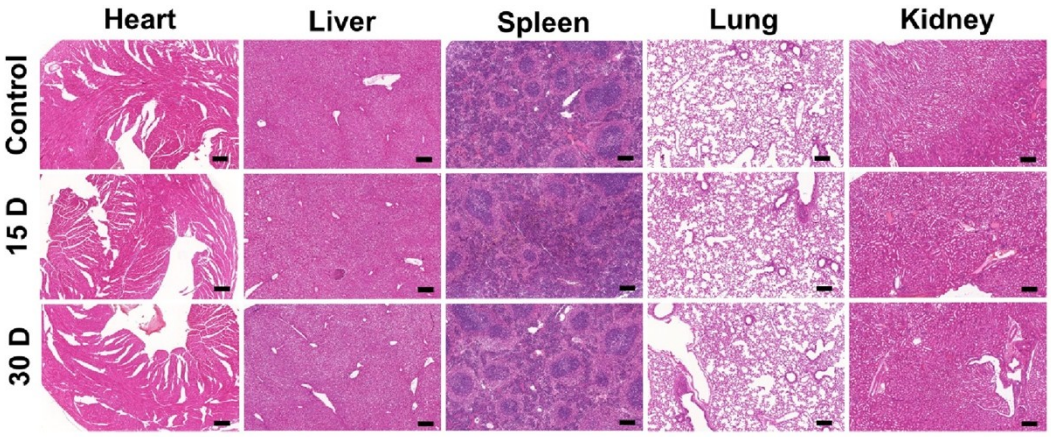

Figure S11. H&E stained main tissues collected from control mouse and mice treated with $NaYF_4$@SiO_2 for 15 and 30 days (scale bar: 200 μm).